ELECTRON OPTICS BASED ON QUADRUPOLE MULTIPLETS FOR DARK FIELD IMAGING AND DIFFRACTION WITH MeV ELECTRON BEAMS

B. Alberdi-Esuain*[,1], T. Kamps[1]
Helmholtz-Zentrum Berlin für Materialien und Energie, Berlin, Germany
[1]also at Humboldt Universität zu Berlin, Berlin, Germany

Abstract

Ultrafast electron probing techniques offer unique experimental tools for investigating the structural dynamics of ultrafast photo-induced processes in molecular and condensed phase systems. In this work, we propose using the SEALAB Photoinjector's exceptional and versatile electron beam parameters to develop a state-of-the-art facility for ultrafast electron diffraction and imaging (UED and UEI) experiments with high sensitivity in space, energy, and time. We first address the design of an electron lens based on quadrupoles that enables easy switching between diffraction and direct imaging modes with minimal system changes. We compare the performance of the quadrupole-based lens with a simpler solenoid-based lens with similar functionality by calculating their respective aberration coefficients. Furthermore, we introduce the necessary beam-line modifications for enabling dark field imaging in the SEALAB Photoinjector. This development is crucial to achieve high-resolution imaging and enable the study of a wide range of material systems.

INTRODUCTION

The SEALAB Photoinjector is a superconducting linear accelerator located at the Helmholtz-Zentrum Berlin. Recent studies have shown that the beamline is versatile enough to produce electron bunches suitable for MeV Ultrafast Electron Diffraction (UED) and Imaging (UEI) experiments. The Photoinjector's combination of spatial and temporal resolution can resolve photo-induced structural dynamics as fast as 100 fs in solid-state targets [1]. The Photoinjector operates in continuous wave mode, with a repetition rate that can be tuned up to 1.3 GHz – a unique feature among UED facilities worldwide [2]. The Photoinjector's MeV range energy also reduces space-charge forces, enabling it to pack more electrons per bunch than lower energy facilities thus providing the opportunity to perform single-shot experiments. The simplified layout of the beamline can be seen in Fig. 1. The electron optics design for UED and UEI is tackled in this work. The goal is to transfer the target information to the detector with the highest quality possible. To do this, the beamline section between the target and detector, with a length of $L \approx 5$ m, will be used. In addition, the optics design aims to attenuate the background signal formed by unscattered electrons that overwhelms the information-carrying electrons by using a beam-blocker placed on a intermediate Fourier plane, the so called dark field mode [3].

* benat.alberdi_esuain@helmholtz-berlin.de

ELECTRON OPTICS

When designing an electron optical system, any lens will introduce aberrations that degrade the quality of the transferred information. However, lenses are necessary for imaging because a drift section cannot provide the necessary phase advance. The goal is to design an optical system composed of lenses that minimize the aberration coefficients. The electron optics in the SRF Photoinjector must meet several requirements. It must provide imaging and diffraction modes at the detector, with an intermediate Fourier plane always placed at the same position in the beamline for both X and Y axes to filter unscattered electrons with a beam-blocker. The magnifications in X and Y must be equal for diffraction and imaging at the final scintillator screen. Additionally, X and Y phase-spaces must be decoupled to conserve directional information of the target. To build such system, at least two lenses are needed. The first one must produce a Fourier plane for both X and Y directions at the the beam-blocker position. The second one must provide different focal lengths for two operation modes to switch between diffraction and imaging modes. The sketch of the electron optics can be seen in Fig. 1. The design of an axisymmetric zooming lens, which can change its focal distance by changing only one of the lens parameters, is tackled first. In light optics, composed lenses can zoom-in and -out by varying the distance between the individual components, but this is not practical in accelerators because the lens components must be precisely positioned to avoid parasitic aberrations. Therefore, a change in intensity through one of the components of the lens must provide different focal distances in which the symmetry between X and Y is conserved.

Axisymmetric Zooming Lens with Quadrupoles

The focusing strength of single quadrupoles scales more favorably with beam energy than the one of solenoids. In addition, properly aligned quadrupoles do not couple X and Y phase-spaces. On the other hand, individual quadrupoles do not constitute axisymmetric lenses since they have the opposite focusing-defocusing effect in both transverse directions. Nevertheless, axisymmetric lenses can be constructed by combining several quadrupoles. To design the electron optics, the quadrupole design seen in Fig. 2, which is already used in SEALAB, is utilized. These are inexpensive air-cooled quadrupoles. The effective length is $l_{\mathrm{eff}} = 119.2$ mm and the distance from the poles to the beam axis is 32 mm. Currents of 8 A through the coils produce a maximum on-axis gradient of 1 T/m, providing a quadrupole strength of approximately $100/\mathrm{m}^2$ for a beam momentum of 3 MeV/c.

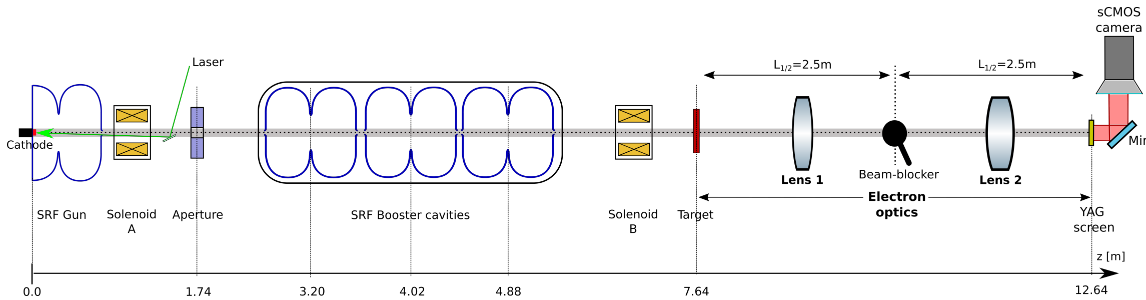

Figure 1: Sketch of the UED beamline in the SRF Photoinjector.

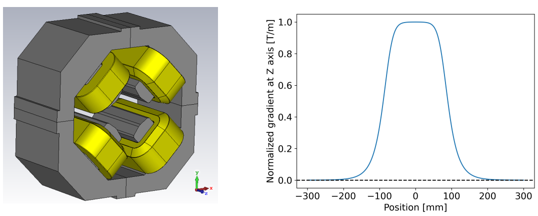

Figure 2: Design (left) and normalized gradient (right) of the SEALAB air-cooled quadrupoles.

Dymnikov et al. studied the composition of quadrupole multiplets that have the same properties as axisymmetric lenses [4]. If R_L is the transfer matrix of the composed lens, it will be axisymmetric only if it has the following shape:

$$\begin{pmatrix} x \\ x' \\ y \\ y' \end{pmatrix} = R_L \begin{pmatrix} x_0 \\ x'_0 \\ y_0 \\ y'_0 \end{pmatrix} = \begin{pmatrix} R_{L11} & R_{L12} & 0 & 0 \\ R_{L21} & R_{L22} & 0 & 0 \\ 0 & 0 & R_{L11} & R_{L12} \\ 0 & 0 & R_{L21} & R_{L22} \end{pmatrix} \begin{pmatrix} x_0 \\ x'_0 \\ y_0 \\ y'_0 \end{pmatrix}.$$

Hence, the 2x2 sub-matrices R_{L-X} and R_{L-Y} must be equal in an axisymmetric lens. This condition is nearly met by Russian multiplets, which consist of an even number of quadrupoles powered symmetrically around the center of the lens: A-B-B-A for a quadruplet, A-B-C-C-B-A for a sextuplet, and so on. The quadrupoles alternate between focusing and defocusing effects (F-D-F-D) and are symmetrical in length and spacing between them ($l_1 - S_1 - l_2 - S_2 - l_2 - S_1 - l_1$). The transfer matrix R_R for Russian multiplets always has the shape

$$\begin{pmatrix} x \\ x' \\ y \\ y' \end{pmatrix} = R_R \begin{pmatrix} x_0 \\ x'_0 \\ y_0 \\ y'_0 \end{pmatrix} = \begin{pmatrix} R_{R11} & R_{R12} & 0 & 0 \\ R_{R21} & R_{R22} & 0 & 0 \\ 0 & 0 & R_{R22} & R_{R12} \\ 0 & 0 & R_{R21} & R_{R11} \end{pmatrix} \begin{pmatrix} x_0 \\ x'_0 \\ y_0 \\ y'_0 \end{pmatrix}.$$

It is possible to find combinations of quadrupole strengths and positions that make the transfer matrix R_R axisymmetric ($R_{R11} = R_{R22}$). The Russian Quadruplet is the simplest multiplet that can do so, but this cannot be achieved for more than one excitation values of any of the quadrupoles, so it cannot work as a zooming lens. The Russian Sextuplet is the simplest system that can act as a zooming axisymmetric lens by changing the excitation of the central quadrupoles. This is possible because R_{R11} and R_{R22} are both quadratic functions of the strength of the middle quadrupoles (K_3) and, by carefully selecting the rest of the sextuplet parameters, both parabolas can intersect for two different values of K_3. In addition to forming an axisymmetric zooming lens, another requirement is that the two working points of the lens provide diffraction ($R_{11} = 0$) and imaging ($R_{12} = 0$) between two points in the beamline separated by a distance $L_{1/2}$. To find a numerical solution that satisfies all of the conditions, Python is used. A function calculates the transfer matrices of the equivalent lens, multiplies them with the transfer matrices of the drifts p and q in front and behind the lens, and then uses a nonlinear equation system solver to find a solution for the free parameters $K_1, K_2, K_3, S_1, S_2, S_3$, p and q that fulfill the previous requirements. The results are then verified with the particle dynamics code Bmad [5]. The raytracing using linear optics can be seen in Fig. 3.

Aberration Coefficients

The quality of a lens is determined by its intrinsic aberration coefficients, which represent deviations from linear optics due to higher order dynamics. However, previous calculations only considered linear optics using hard-edge models of the quadrupoles. To address this, the gradient on axis of the quadrupoles shown in Fig. 2 is implemented into the particle tracking code Astra [6] to calculate the aberration coefficients for both the diffraction and imaging operation modes of the sextuplet lens [7]. The performance of the sextuplet lens is then compared with a simpler solenoid lens, composed of two consecutive solenoids with opposite field values to cancel out the Larmor rotation and the coupling between X and Y. The position and strength of the solenoid doublets is chosen so that the composed solenoid lens provides the same magnifications for diffraction and imaging as the sextuplet lens. The field map of Solenoid B from Fig. 1 is used for the tracking. The results are shown in Table 1. The divergence of the calculated aberration coefficients $\langle x|x_0\rangle$ and $\langle y|y_0\rangle$ from the R_{11} and R_{12} values of Fig. 3 show that deviations from the linear optics occur once real fields are used for tracking. It can also be seen that spherical aberrations are dominant in the optical system, and that quadrupole-based optics offers significantly reduced spherical aberrations compared to solenoid-based optics with the same functionality. It has to be mentioned that only the intrinsic aberrations have been used to compare the lenses, not parasitic aberrations.

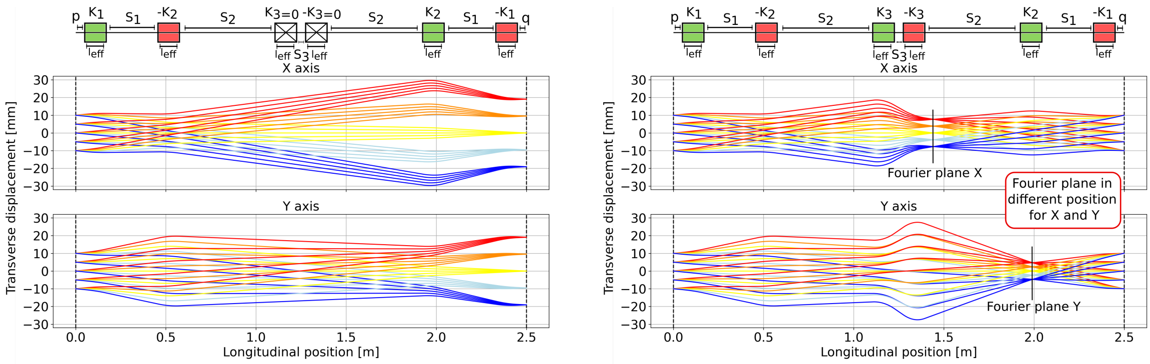

Figure 3: The linear trajectories for a Russian Sextuplet which can switch between diffraction (left) and imaging (right) modes by changing only the strength of the central quadrupoles from $K_3 = 0.0/m^2$ to $K_3 = 33.57/m^2$. The rest of the parameters are $K_1 = 8.65/m^2$, $K_2 = 11.20/m^2$, $S_1 = 0.29$ m, $S_2 = 0.53$ m, $S_3 = 0.05$ m and p = q = 0.05 m. The colors of the trajectories represents the initial divergence. In the case of diffraction(imaging), $R_{11} = 0.0(-1.0)$ and $R_{12} = 1.9(0.0)$.

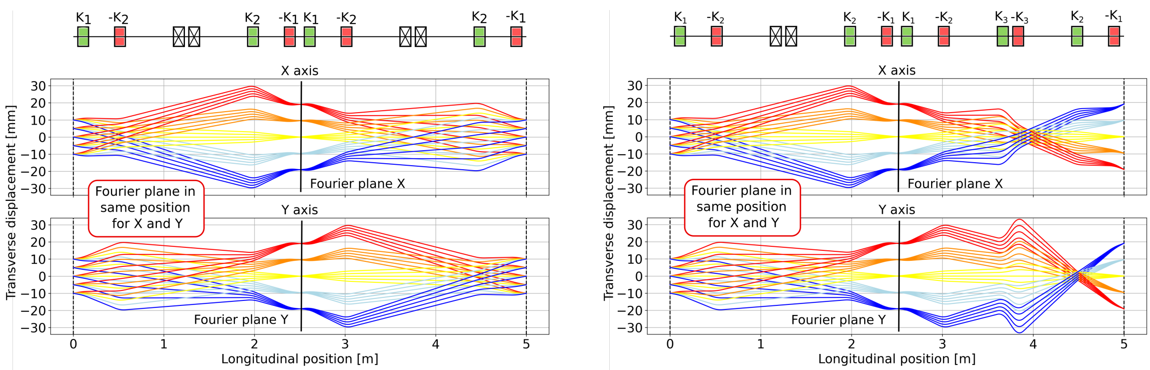

Figure 4: Dark field modes for imaging (left) and diffraction (right). The X axis in these plots is two times the ones in Fig. 3.

Table 1: Aberration coefficients of the quadrupole- and solenoid-based lenses with $\theta = x'$, $\phi = y'$ and $\delta = \frac{\Delta p_z}{p_z}$ [7].

	Aberration Coefficient		Quad. Diff.	Sol. Diff.	Quad. Imag.	Sol. Imag.
	$<x\|x_0>$		1.91	1.92	0.10	0.08
	$<y\|y_0>$		1.91	1.92	0.10	0.08
	$<x\|x'_0>$	[m/rad]	0.02	0.04	-0.97	-0.94
	$<y\|y'_0>$	[m/rad]	0.03	0.04	-0.89	-0.94
Chromatic	$<x\|\theta_0\delta_0>$	[m/rad]	-1.11	-1.15	5.95	6.6
	$<y\|\phi_0\delta_0>$	[m/rad]	2.1	2.1	5.22	5.7
	$<x\|x_0\delta_0>$	[m/rad]	1.63	2.78	1.52	5.28
	$<y\|y_0\delta_0>$	[m/rad]	3.87	2.78	6.3	5.28
Spherical	$<x\|\theta_0^3>$	[m/rad^3]	0.48	-42.85	-7.06	-770.21
	$<y\|\phi_0^3>$	[m/rad^3]	0.31	-42.85	-7.38	-770.21
	$<x\|\theta_0\phi_0^2>$	[m/rad^3]	-34.85	-42.85	-345.88	-770.22
	$<y\|\theta_0^2\phi_0>$	[m/rad^3]	-64.08	-42.85	-344.00	-770.22

Design for Dark Field Imaging and Diffraction

The design of a beamline for dark field imaging and diffraction using two consecutive units of the axisymmetric lens design is proposed here. In the first half, the axisymmetric lens is always used in diffraction mode (the two middle quads can be removed) to produce a Fourier plane in the middle of the optical beamline for both X and Y. The unscattered electrons can be blocked using a beam blocker inserted at this position. In the second half of the beamline, the same lens is used, but this time with the capability of doing diffraction and imaging. As the transfer matrix of both lenses is equal when operating in diffraction mode, the Fourier transformation of the intermediate Fourier plane produces an image of the target at the detector, while the image of the intermediate Fourier plane produces a diffraction pattern at the screen as shown in Fig. 4.

CONCLUSIONS

In this work, we have designed an axisymmetric electron lens composed of quadrupoles that can switch between diffraction and imaging modes by changing a single power supply value. In addition, a dark field imaging mode has been developed for the requirements of the SRF Photoinjector in SEALAB. Both the quadrupole and solenoid solutions require only three independent power supplies for the dark field optics. A drawback of the quadrupole-based dark field optical system designed here is that the magnification of the imaging mode is always -1. Therefore, an additional imaging lens system would be required after the detector to achieve any meaningful magnification. Fortunately, there is sufficient space behind the SRF Photoinjector to add some meters of beamline for magnification optics after which a second detector could be added.

REFERENCES

[1] B. Alberdi Esuain, J. G. Hwang, A. Neumann, and T. Kamps, "Novel approach to push the limit of temporal resolution in ultrafast electron diffraction accelerators", *Sci. Rep.*, vol. 12, p. 13365, 2022. doi:10.1038/s41598-022-17453-z

[2] D. Filippetto, P. Musumeci, R. K. Li, *et al.*, "Ultrafast electron diffraction: Visualizing dynamic states of matter", *Rev. Mod. Phys.*, vol. 94, p. 045004, 2022. doi:10.1103/RevModPhys.94.045004

[3] Z. Zheng, D. Yingchao, C. Shuchun, *et al.*, "Experiments on bright-field and dark-field high-energy electron imaging with thick target material", *Phys. Rev. Accel. Beams*, vol. 21, p. 074701, 2018. doi:10.1103/PhysRevAccelBeams.21.074701

[4] A. D. Dymnikov, G. A. Glass, and B. Rout, "Zoom quadrupole focusing systems producing an image of an object", *Nucl. Instrum. Methods Phys. Res., Sect. B*, vol. 241, p. 402, 2005. doi:10.1016/j.nimb.2005.07.049

[5] D. Sagan, "Bmad: A relativistic charged particle simulation library", *Nucl. Instrum. Methods Phys. Res., Sect. A*, vol. 558, p. 356, 2006. doi:10.1016/j.nima.2005.11.001

[6] K. Floettmann, "ASTRA — A Space Charge Tracking Algorithm", 2007. https://www.desy.de/mpyflo

[7] G. W. Grime, F. Watt, G. D. Blower, J. Takacs, and D. N. Damieson, "Real and parasitic aberrations of quadrupole probe-forming systems", *Nucl. Instrum. Methods Phys. Res.*, vol. 197, pp. 97-109, 1982. doi:10.1016/0167-5087(82)90123-5